This full text paper was peer reviewed at the direction of IEEE Communications Society subject matter experts for publication in the ICC 2007 proceedings.

Equivalent-Capacity-Based Design of Space-Time Block-Coded Sphere-Packing-Aided Multilevel Coding

R. Y. S. Tee, O. Alamri, S. X. Ng and [1]L. Hanzo

School of ECS, University of Southampton, SO17 1BJ, UK.
Email: [1]lh@ecs.soton.ac.uk, http://www-mobile.ecs.soton.ac.uk

Abstract – **A multilevel coding (MLC) scheme invoking sphere packing (SP) modulation combined with space time block coding (STBC) is designed. The coding rates of each of the MLC component codes are determined using the so-called equivalent capacity based constituent-code rate-calculation procedure invoking a 4-dimensional (4D) sphere packing bit-to-symbol mapping scheme. Four different-rate Low-Density Parity Check (LDPC) constituent-codes are used by the MLC scheme. The performance of the resultant equivalent capacity based design is characterized using simulation results. Our results demonstrate an approximately 3.5dB gain over an identical scheme dispensing with SP modulation. Furthermore although a similar performance gain is attained by both the proposed MLC scheme and its benchmarker, which uses a single-class LDPC code, the MLC scheme is preferred, since it benefits from the new classic philosophy of using low-memory, low-complexity component codes as well as providing an unequal error protection capability.**

1. INTRODUCTION

Coded modulation is based on jointly designed coding and modulation where the parity bits are accommodated by expanding the modulated signal constellation, rather than by expanding the bandwidth required. An attractive example of coded modulation, namely multilevel coding (MLC) was proposed by Imai and Hirawaki [1], which protects each bit of a non-binary symbol with the aid of different-rate binary codes. An attractive iterative multistage decoding (MSD) scheme was also proposed in [1] for attaining a high decoding performance at a low decoding complexity. In this MSD structure, the ith bit constituting a specific protection class associated with the constituent code C^i is decoded by the i^{th} decoder, while simultaneously exploiting the $a\ priori$ information obtained from the demodulator, before passing the information to the $(i+1)$st protection level associated with the constituent code C^{i+1}. This MSD process is activated level by level at each different-rate component decoder, each of which constitutes a flexible component code that has numerous configurable parameters. The explicit advantage of having independently configurable parameters for the low-complexity component codes is that they may be appropriately adjusted for diverse applications.

In this paper, we employ a novel sphere packing (SP) modulation scheme combined with orthogonal transmit diversity design, which was introduced by Su $et\ al.$ [2]. Various 2-dimensional (2D) bit-to-symbol mapping schemes have been investigated in [3] [4] and [5] with the motivation of improving the achievable bit error rate (BER) performance of MLC schemes with the aid of diverse bit-to-SP-symbol mapping strategies. In contrast to Alamouti's independently modulated symbols transmitted within the two consecutive timeslots and two antennas [6], here we invoke a multidimensional SP strategy, where SP modulation is used for jointly designing the symbols transmitted within the consecutive time-slots of the Space Time Block Codes (STBC) invoked for transmission over Rayleigh fading channels. Historically speaking, the STBC concept of Alamouti [6] was then further generalized by Tarokh $et\ al.$ [7], but again, no attempt was made in [6] and [7] to jointly optimize the space-time signal design of the two consecutive time-slots and two antennas, although we will demonstrate that this results in substantial performance benefits. This is expected, because it is the joint space-time-symbol error probability that we would like to minimize for the sake of increasing the system's integrity in fading channels.

The sphere packing aided concatenated design of STBCs [8] was further developed by Alamri $et\ al.$ [9] by invoking an iterative turbo receiver. Motivated by the substantial performance improvements reported in [9], in this treatise we combine the SP concept with a MLC scheme for the sake of creating an improved orthogonal transmit diversity design. The minimum Euclidean distance of symbols defined in an M-dimensional (MD) space may be maximized by finding the most meritorious mapping of the bits to the signalling constellation. It is worth noting, however that the choice of the best mapping typically depends on the channel conditions, as exemplified by the now classic Trellis Coded Modulation (TCM), arrangement designed for Gaussian channels [10], by Bit-Interleaved Coded Modulation (BICM) schemes proposed for Rayleigh channels [10] or by the design of [9]. The MD modulated symbols are then fed into the STBC encoder. We term this scheme as a Space-Time Sphere Packed Multilevel Coded Modulation (STBC-SP-MLC) arrangement.

A beneficial technique devised for determining each component code's rate in MLC was detailed by Wachsmann $et\ al.$ in [11], where the design concept exploited the so-called chain-rule of mutual information introduced in [12] as it will be detailed in Section 3. To elaborate a little further, the authors of [11] applied the equivalent capacity rules both to conventional one-dimensional and to two-dimensional modulated signal constellations. In this paper, we will further extend the concepts proposed in [11] for improving the design of our STBC-SP-MLC scheme, invoking a 4-dimensional SP constellation. More explicitly, the equivalent capacity design [11] will be further developed for determining the optimum LDPC constituent code rates of the STBC-SP-MLC scheme in conjunction with various bit-to-SP-symbol mapping strategies in the 4D SP space. The BER performance of both the individual MLC protection classes as well as of the combined MLC scheme invoking the optimum LDPC coding rates will be evaluated by simulations.

The rest of this contribution is organized as follows. Section 2 provides an overview of our system, outlining our SP aided iterative MSD assisted MLC based decoder. The proposed equivalent capacity based design of the STBC-SP-MLC scheme is detailed in Section 3. Section 4 quantifies the achievable performance of this novel scheme, invoking the equivalent capacity based coding rates, while our conclusions are presented in Section 5.

2. SYSTEM OVERVIEW

The schematic of the proposed STBC-SP-MLC arrangement is shown in Figure 1. The binary source bit stream u is serial-to-parallel (S/P) converted at the transmitter. The four individual source bits, namely u^1, u^2, u^3, u^4, are protected by four different-rate MLC encoders, as

The financial support of the EPSRC, UK, Ministry of Higher Education of Saudi Arabia and that of the European Union under the auspices of the Phoenix and Newcom projects is gratefully acknowledged.

1-4244-0353-7/07/$25.00 ©2007 IEEE

seen in Figure 1. The output bits of encoder C^i, $i = 1...4$, having a total encoded frame length of n bits are denoted as b^i=$b^i_1, b^i_2, ..., b^i_n$.

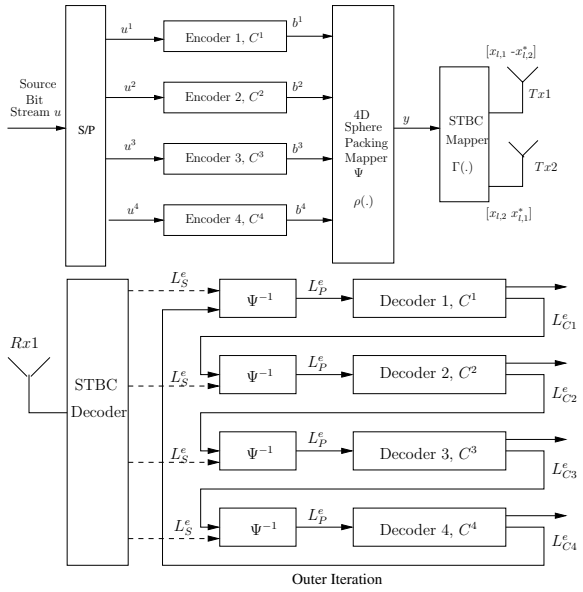

Figure 1: The Space-Time Block-Coded Sphere Packing aided Multilevel coding (STBC-SP-MLC) scheme.

Again, we employ LDPC component codes owing to their powerful error correcting capability, low complexity and flexible coding rates. The random nature of the parity check matrix construction of LDPC codes allows us to dispense with the employment of additional channel interleavers. Each LDPC codeword is decoded using the belief propagation algorithm [13]. The MLC encoded bit stream is then forwarded to the sphere packing modulator ψ of Figure 1. Our 4D SP modulator has L=16 constellation points. Since there are 24 immediately adjacent neighbours having different Euclidean distances in the 4D SP constellation [14], we use that specific set of 16 points out of the entire set of 24, which exhibits the maximum Euclidean distance.

The 4D SP phasor points are denoted as S=$(a_{l,1}, a_{l,2}, a_{l,3}, a_{l,4})$, where we have l=$0, 1, 2, ..., L-1$. Here we would like to represent the four individual coordinates of S in the 4D SP-space using real values, while satisfying the SP-constraint of $(a_1 + a_2 + a_3 + a_4)$=k, where k is an even integer constant [14]. The total energy of the signal points is represented by $E \triangleq \sum_{l=0}^{L-1}(|a_{l,1}|^2+|a_{l,2}|^2+|a_{l,3}|^2+|a_{l,4}|^2)$ [9].

After SP-modulation, the 4D SP symbol is mapped to two complex-valued 2-bit symbols, before being fed into a STBC scheme using two transmit antennas. The bit-to-symbol mapping function of the system is denoted as [9]

$$\begin{aligned}\Gamma(\rho(b^1, b^2, b^3, b^4)) &= \Gamma(a_{l,1}, a_{l,2}, a_{l,3}, a_{l,4}),\\ &= \{a_{l,1} + ja_{a,2}, a_{l,3} + ja_{l,4}\},\\ &= \{x_{l,1}, x_{l,2}\}, \end{aligned} \quad (1)$$

where $\rho(.)$ is the SP function used for mapping the original input bits to the SP symbols and $\Gamma(.)$ represents the mapping of the 4D SP symbols to the complex-valued 2-bit symbols $x_{l,1}$ and $x_{l,2}$ after STBC encoding. The throughput of the overall system is $\log_2 L/2$, since each SP symbol is transmitted over two antennas in two consecutive time slots. When taking into account the employment of rate-r channel coding, the effective throughput becomes $1/r.\log_2 L/2$.

Figure 1 also shows the receiver of the system, where a STBC decoder equipped with a single receive antenna is employed. The STBC decoder forwards its complex-valued symbols to the SP-demodulator ψ^{-1} of Figure 1 and the resultant bits are then decoded at the different-protection LDPC decoders in an iterative MSD manner. At the initial stage, the SP-demodulator ψ^{-1} of Figure 1 only receives the channel's output information represented in terms of Log-Likelihood Ratios (LLR) L^e_S from the STBC decoder. The $extrinsic$ LLRs L^e_P of Figure 1 produced by the SP-demodulator are fed into the level-1 decoder of C^1, which then outputs a set of corresponding $extrinsic$ LLRs L^e_{C1} to the demodulator. This LLR provides useful $a\ priori$ information for the SP demodulator, where the LLRs gleaned from the previous protection level are updated. As the decoding process continues, each MSD level receives useful $a\ priori$ LLRs from the previous MSD level, which can be exploited in the LDPC decoder. The next outer iteration seen in Figure 1 commences, when the LLR information of the SP-demodulator has been updated with the $extrinsic$ information received from all MSD levels.

Alamri $et\ al.$ [9] showed that the SP symbol $\mathbf{r}$ received by the STBC decoder can be written as

$$\mathbf{r} = h \cdot \sqrt{\frac{2L}{E}} \cdot \mathbf{s}^l + \mathbf{w}, \quad (2)$$

where we have $h = (|h_1|^2 + |h_2|^2)$ and h_1 as well as h_2 represent the channel impulse response (CIR) corresponding to the first and second transmit antennas. Furthermore, we have $\mathbf{s}^l \in S, 0 \leq l \leq L-1$, and $\mathbf{w}$ is a 4D real valued Gaussian random variable having a covariance matrix of $\sigma_w^2 \cdot \mathbf{I}_{N_D} = h \cdot \sigma_n^2 \cdot \mathbf{I}_{N_D}$. The subscript of N_D=4 indicates that the symbol constellation S is four-dimensional and $\mathbf{I}_{N_D}$ is a (N_DxN_D)-dimensional identity matrix.

The max-log approximation of the $extrinsic$ LLR of a single bit b_k output by the demodulator can be expressed as

$$\begin{aligned} & L(b_k|r) - L_a(b_k)\\ = \ & max_{\mathbf{s}^l \in S_1^k}\left[-\frac{1}{2\sigma_w^2}(\mathbf{r} - \alpha \cdot \mathbf{s}^l)(\mathbf{r} - \alpha \cdot \mathbf{s}^l)^T + \sum_{j=0, j\neq k}^{B-1} b_j L_a(b_j)\right]\\ - \ & max_{\mathbf{s}^l \in S_0^k}\left[-\frac{1}{2\sigma_w^2}(\mathbf{r} - \alpha \cdot \mathbf{s}^l)(\mathbf{r} - \alpha \cdot \mathbf{s}^l)^T + \sum_{j=0, j\neq k}^{B-1} b_j L_a(b_j)\right], \end{aligned} \quad (3)$$

where the SP symbols carry B number of MLC bits, $\mathbf{b} = b_{0,...,B-1} \in \{0, 1\}$. Let us assume furthermore that S_1^k and S_0^k represent two specific 2D subsets of the 4D SP symbol constellation S, which obey $S_1^k \triangleq \{\mathbf{s}^l \in S : b_k = 1\}$ and $S_0^k \triangleq \{\mathbf{s}^l \in S : b_k = 0\}$, respectively.

In general, for a MLC scheme having q protection levels, the MLC-encoded bits are mapped to a total of N=2^q possible SP symbols. The updated $a\ priori$ LLRs obtained from the preceding MLC protection-level at level $i = 1...4$ are given by $L^e_{Ci} \triangleq \{L_a(b_k); k \in \{tq + (i-1), t = 0, 1, ..., N\}\}$.

3. EQUIVALENT CAPACITY DESIGN

The calculation of channel capacity is based on the maximization of mutual information over all the relevant parameters, where the capacity of a particular channel can be formulated as $C = \max_{p(S_i)} I(Y; S)$. We then apply the so-called chain-rule of mutual information [11] as follows

$$\begin{aligned} I(Y; S) &= I(Y; b^1, b^2, ..., b^l)\\ &= I(Y; b^1) + I(Y; b^2|b^1) + ...\\ &\quad + I(Y; b^l|b^1, b^2, ..., b^{l-1}), \end{aligned} \quad (4)$$

where Y denotes the legitimate received signal set, S represents the legitimate transmitted symbol set and b^i, $i = 1...4$, denotes the individual binary bits of the different protection levels.

Let us now consider the proposed STBC-SP-MLC scheme invoking 4D SP modulation. Each 4D SP symbol is mapped to the complex-valued symbols $x_{l,1}$ and $x_{l,2}$, before being mapped to the two consecutive timeslots using two transmit antennas, as shown in

Figure 1. The resultant signal is then transmitted over a correlated Rayleigh fading channel. Therefore each of the STBC symbols becomes two-dimensional and has an unequal probability for the resultant signal constellation points, as it will be shown in the context of Table 1, once our discourse has reached a sufficiently detailed stage. The partitioning of the 4D SP constellation is exemplified in Figure 2 for the conceptually simpler stylized 1D scenario of 16-level Amplitude Shift Keying (16-ASK). The partitioning of the signal set S can be further divided into two parts, resulting in the subsets of $S(b^1 = 0)$ and $S(b^1 = 1)$, each containing a total of eight out of the $L = 16$ symbols. In each subset, for example at the ith level of the subset $S(b^1) = 0$, the 8-symbol constellation segment can be further subdivided into the two 4-symbol subsets of $S(b^1 = 0, b^2 = 0)$ and $S(b^1 = 0, b^2 = 1)$ at level $(i + 1)$, etc. The partitioning tree of the signal set is completed, when the partitioned SP-constellation contains only a single symbol at level l. Please note again that in Figure 2 we used a simplified 1D 16ASK constellation for the sake of conceptual simplicity, since the 4D SP space cannot be readily portrayed graphically.

For a 2D STBC scheme, having $N_t = 2$ transmitter and $N_r = 1$ receiver antennas, the signal Y received at the single antenna, can be represented as [15]

$$Y = \sum_{j=1}^{N_t} |h_j|^2 X + \Omega = \chi^2_{2Nt} S + \Omega, \tag{5}$$

where X is the 2D complex-valued received signal, h_j represents the complex-valued Rayleigh fading coefficient and χ^2_{2Nt} represents a chi-squared distributed random variable having $2N_t$ degrees of freedom. Furthermore, Ω denotes the resultant equivalent noise at the STBC receiver having zero mean and a variance of $\chi^2_{2N_t} N_0/2$ per dimension, where $N_0/2$ is the original noise variance per dimension.

For the STBC-SP-MLC system of Figure 1 characterized in Equation 5, which receives two complex-valued STBC symbols of the signal Y and transmits the M-ary 2D STBC signals $X_m, m \in \{1, 2, ..., M\}$, over the two STBC antennas in two consecutive timeslots, the corresponding conditional probability is given by

$$p(Y|X_m) = \frac{1}{\pi N_0 \chi^2_{2N_t}} \exp\left(\frac{-|Y - \chi^2_{N_t} X_m|^2}{\chi^2_{2N_t} N_0}\right). \tag{6}$$

We consider the occurrence of all legitimate transmitted M-ary signals X_m having a probability of $p(X_m)$ for $m \in \{1, 2, ..., M\}$, where the mutual information between Y and X_m [12] can be expressed as

$$\begin{aligned} I(X_m; Y) &= \sum_{m=1}^{M} \int_Y p(X_m, Y) \log_2\left(\frac{p(X_m, Y)}{p(X_m)p(Y)}\right) dY \\ &= \sum_{m=1}^{M} \int_Y p(Y|X_m) p(X_m). \\ &\quad \log_2\left(\frac{p(Y|X_m)}{\sum_{n=1}^{M} p(Y|X_n)p(X_n)}\right) dY. \end{aligned} \tag{7}$$

Expressing the mutual information with the aid of the entropy as $I(X;Y) = H(X) - H(X|Y)$, we arrive at

$$\begin{aligned} I(X;Y) &= -\sum_{m=1}^{M} p(X_m) \log_2(p(X_m)) \\ &\quad - \sum_{m=1}^{M} p(X_m) E\left[\log_2\left(\sum_{n=1}^{M} \exp(\psi_{m,n})\right) |X_m\right] \end{aligned} \tag{8}$$

where we have $\psi_{m,n} = \frac{-|\chi^2_{2N_t}(X_m - X_n) + \Omega|^2 + |\Omega|^2}{\chi^2_{2N_t} N_0}$, while $E[A|X_m]$ is the expectation of A conditioned on X_m.

Since the STBC-SP-MLC scheme invokes a single receive and two transmit antennas, there are two modulated STBC symbols, each gleaning the amount of mutual information quantified by Equation 8. The total mutual information between a transmitted 4D SP symbol and the received 4D SP symbol is the average of that of the two 2D STBC symbols expressed as follows

$$I(S;Y) = \frac{I^1(X^1;Y^1) + I^2(X^2;Y^2)}{2}, \tag{9}$$

where I^i denotes the mutual information between the i^{th} transmitted STBC signal Y^i and the M-ary 2D received signal X^i, $i \in \{1, 2\}$. The information gleaned at the MLC protection level i can be calculated from the chain rule of Equation 4 according to [11] [1]

$$\begin{aligned} I(Y; b^i|b^1...b^i - 1) &= I(Y; b^i...b^{l-1}|b^1...b^{i-1}) \\ &- I(Y; b^{i+1}...b^{l-1}|b^1...b^i). \end{aligned} \tag{10}$$

4. SIMULATION RESULTS

In this section we embark on quantifying the equivalent capacity for the sake of determining the corresponding coding rate of each of the four LDPC protection classes for our proposed STBC-SP-MLC scheme outlined in Figure 1, when communicating over a Rayleigh fading channel having a normalized Doppler frequency of $f_D.T$=0.1. We set the total effective throughput of the system after taking into account a code-rate of 0.5 to 1 bit/channel use, corresponding to 4 bit/SP-symbol for our twin-antenna design and construct benchmarkers having the same effective throughput for comparison. The SP signal constellation points D_4 having the maximum Euclidean distance between adjacent or nearest-neighbour points at a given energy are shown in Table 1.

Symbol	a_1	a_2	a_3	a_4	Symbol	a_1	a_2	a_3	a_4
S_0	0	-1	-1	0	S_8	0	+1	+1	0
S_1	-1	-1	0	0	S_9	+1	+1	0	0
S_2	-1	0	0	-1	S_{10}	+1	0	0	+1
S_3	0	0	-1	-1	S_{11}	0	0	+1	+1
S_4	0	-1	+1	0	S_{12}	0	+1	-1	0
S_5	-1	+1	0	0	S_{13}	+1	-1	0	0
S_6	-1	0	0	+1	S_{14}	+1	0	0	-1
S_7	0	0	-1	+1	S_{15}	0	0	+1	-1

Table 1: The bit-to-SP-symbol mapping scheme maximizing the Euclidean distance between points, while maintaining the lowest possible energy. The corresponding modulated constellation is seen in Figure 3.

Figure 3 shows the resultant constellation point set of the STBC scheme's 2D constellation mapper. The number seen above each constellation point indicates the probability of occurrence for each point, where the legitimate values of $a_1...a_4$ in the signal space of Table 1 are constrainted to the various combinations of the values ($\pm$1,$\pm$1,0,0) according to our 4D SP space D_4 [14]. For example, $[a_1\ a_2\ a_3\ a_4]$=[$\pm$1 $\pm$1 0 0] or other alternative combinations as shown in Table 1. To elaborate a little further, when each SP symbol is mapped to two complex-valued 2D STBC symbols, they can be represented as $(a_1 + ja_2, a_3 + ja_4)$ according to Equation 1. Again, each of the variables a_1, a_2, a_3 and a_4 may assume one of three possible values, namely $\pm$1, $\pm$1 and 0, although recall that we selected the specific 16 combinations out of the 24 possible combinations, which maximize the Euclidean distance at a given average energy. Again, the SP symbols for all $L = 16$ constellation points are specified in Table 1.

The STBC symbol $(a_1 + ja_2)$ of Equation 1 is mapped to the 1^{st} STBC transmitter of Figure 1, while $(a_3 + ja_4)$ is mapped to 2^{nd} transmitter. All the legitimate combinations of the (a_1, a_2) and

[1] The information provided by the bits of a non-binary symbol for each other may be interpreted as additional auxiliary information provided by a fictitious channel also termed as the equivalent channel in [11]

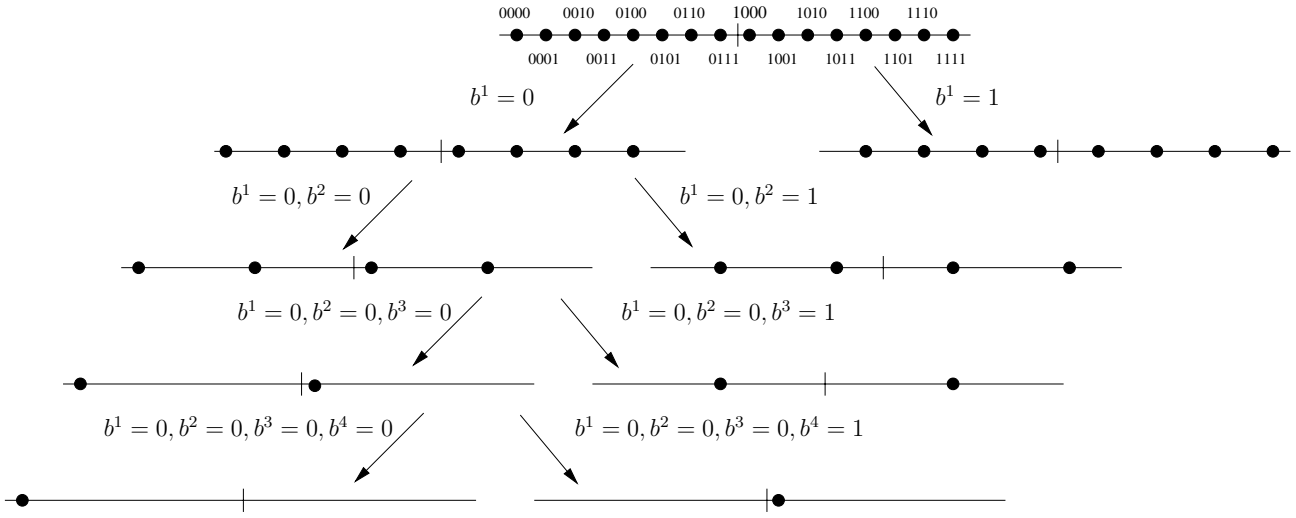

Figure 2: 16-ASK signal partitioning.

(a_3, a_4) values are plotted in Figure 3. We have a total of nine visibly different legitimate constellation points in Figure 3, because some of the points are identical as suggested by the associated doubled or quadrupled probability of occurence. For example, observe in Table 1 that the probability of the constellation point (-1,0), which is given by S_2 and S_6 of the first transmitter, is calculated as 2/16=0.125. Similarly, the probability of occurencefor all the specific constellation points is indicated by the number written above each point in Figure 3 and 4.

At the next MLC protection level, namely level 2, the signal representing the first STBC symbol of transmitter 1 is shown in Figure 4a and 4b. The resultant 5-point subsets $S(b^1 = 0)$ and $S(b^1 = 1)$ provide us with a partition tree of $S(0b^2...b^l)$ and $S(1b^2...b^l)$. Given the knowledge of bit b^1 at level 2, which identifies one of the two partitions seen in Figure 4, we obtain the partitioning of $S(b^2...b^l|b^1)$ at level 2 of the first transmitter. The two branches resulting from this partitioning yield the five unequal-probability constellation points shown in Figure 4.

The partitioning process continues from level 1 to level l. Since in the context of MSD we assume having virtually independent channels for each protection level, the mutual information inferred at each protection level i can be calculated from Equations 8, 9 and 10.

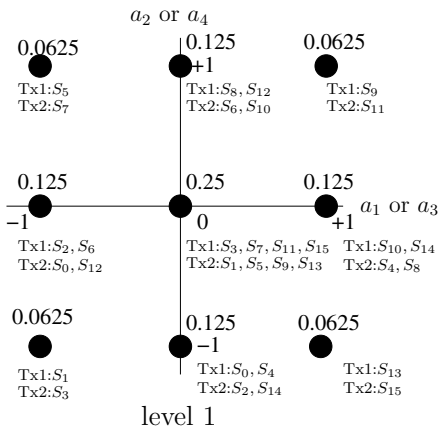

Figure 3: The STBC constellation points at level 1. The number above the dots indicate the probability of occurrence for the symbols, while the symbol indices at the bottom indicate the specific symbol. The first and second transmitter are represented by Tx1 and Tx2, respectively.

The overall effective system throughput of our proposed STBC-SP-MLC scheme is given by

$$R_{sys} = \frac{\sum_{i=1}^{i=q} k_i}{\sum_{i=1}^{i=q} n_i} \cdot \frac{N_{sym}.bps_{sp}}{T_r}, \quad (11)$$

where k_i and n_i denote the number of source bits and encoded bits of the individual MLC component codes, T_r is the total number of STBC timeslots used for transmitting the associated pairs of symbols, while N_{sym} is the number of SP symbols at the input of the STBC encoder in a particular time slot. Finally, bps_{sp} is defined as the number of bits per SP symbol.

Each LDPC component code has an output block length of 640 bits and their resultant combined MLC coding rate is 0.49609($\approx$1/2). We fix our overall effective system throughput after 1/2-rate coding to 1 bit/channel use. Observe in Equation 11 that the throughput of the SP-STBC scheme using no channel coding would be 2 bit/symbol.

Figure 5 shows the equivalent capacity curves detailed in Section 3. The vertical dashed line recorded for the throughput of 2 bit/symbol is used for determining the equivalent capacity for each protection level of the MLC scheme. Since the total throughput of the SP-STBC arrangement is 2 bit/symbol, the throughput of the individual different-protection subchannels will sum up to be the same as the overall SP-STBC scheme's throughput. According to [11], the vertical dashed line that cuts through all the equivalent subchannel capacity curves determines the equivalent-capacity-based coding rate of each component LDPC code. The coding rates determined from the equivalent capacity rules outlined at the end of Section 3 are (0.3478, 0.3043, 0.7174, 0.6413) and the actual LDPC code rates used are shown in Table 2.

A total of 5000 frames containing 2560 MLC-encoded bits were transmitted for the sake of our BER evaluation. Our benchmarker is based on a STBC-MLC structure, which is constituted by the direct serial concatenation of STBC and MLC with conventional 16QAM modulation. The STBC employs two transmit antennas, a single receive antenna and the MLC maps the output symbols into a 2D 16QAM Ungerböck Partitioning (UP) based modulator. The LDPC coding rates for this STBC-MLC UP 16QAM benchmarker are also shown in Table 2, which were obtained by applying the capacity rules derived for UP-aided 16QAM at a code rate of 1/4 in [4].

Figure 6 compares the attainable BER performance of the proposed STBC-SP-MLC scheme to that of the STBC-MLC benchmarker. The conventional MLC scheme does not perform well in a Rayleigh fading channel [5], although the spatial diversity gain provided by a serially concatenated STBC scheme usefully improves its BER performace. However, even this improved performance can be signifi-

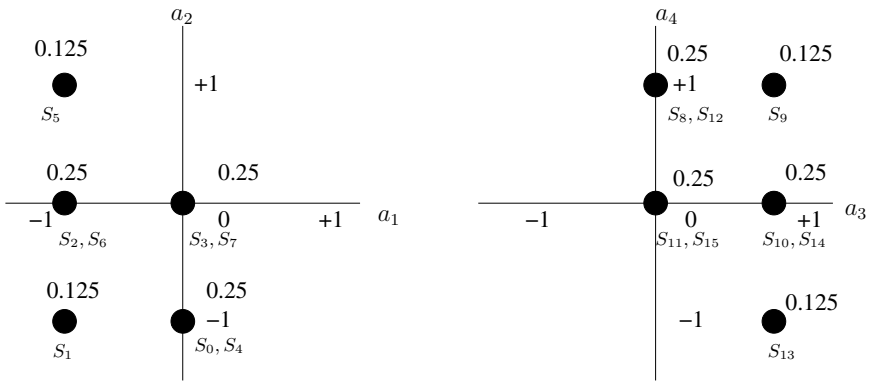

(a) level 2 , b^1=0 (b) level 2, b^1=1

Figure 4: The constellation points of the first STBC transmitter Tx1 at MLC level 2. The number above the dots indicate the probability of occurrence for the symbols, while the symbol indices at the bottom indicate the specific symbol.

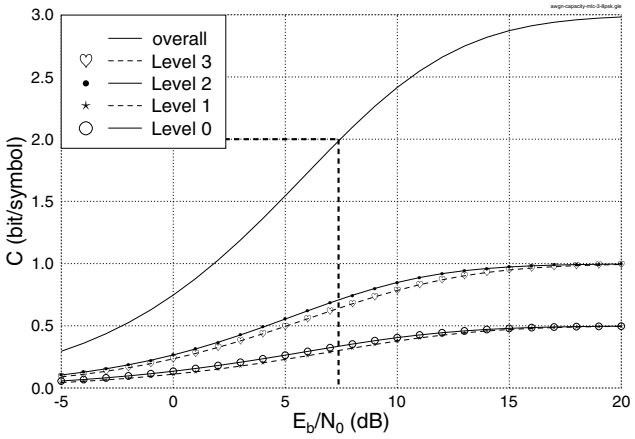

Figure 5: The equivalent capacity curves of the proposed SP-STBC scheme communicating over correlated Rayleigh fading channels where a STBC scheme having N_t=2 and $N_r = 1$ antennas was used.

Coding rate	R_1	R_2	R_3	R_4
STBC-SP-MLC	221/640	193/640	458/640	408/640
STBC-MLC	48/640	228/640	84/640	280/640

Table 2: Coding rates of STBC-SP-MLC and STBC-MLC schemes.

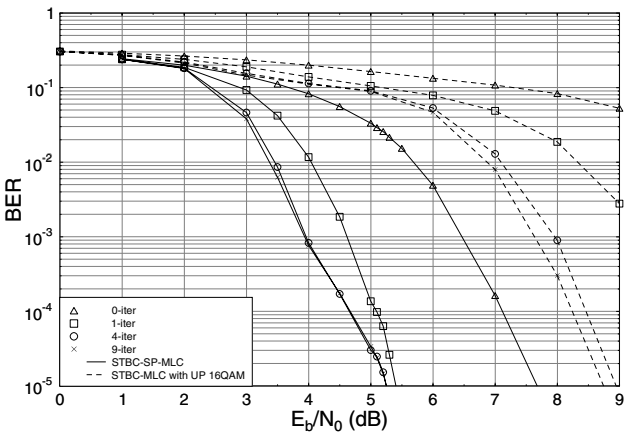

Figure 6: BER versus E_b/N_o performance of the STBC-MLC 16QAM scheme at an effective throughput of 1 bit/symbol using Ungerböck Partitioning (UP) based bit-to-symbol mapping and our proposed STBC-SP-MLC scheme, when communicating over a correlated Rayleigh channel having a Doppler frequency of 0.1. All other parameters are summarized in Table 2 and 3.

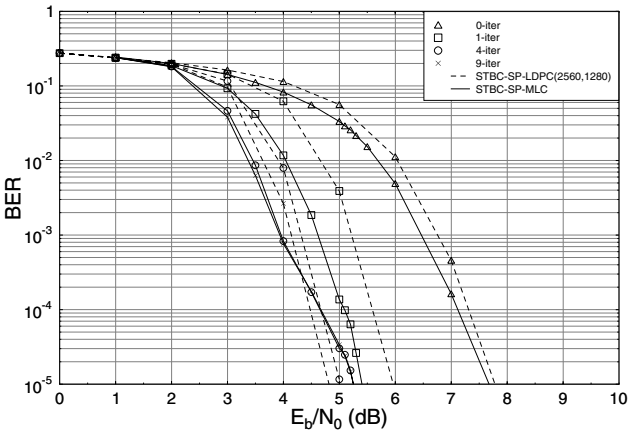

Figure 7: BER versus E_b/N_o performance of the proposed STBC-SP-LDPC scheme using a single 1/2-rate component code LDPC(2560,1280) and having an effective throughput of 1 bit/channel use in comparison to the proposed STBC-SP-MLC scheme, when communicating over a correlated Rayleigh fading channel.All other parameters are summarized in Table 2 and 3.

cantly enhanced with the aid of the proposed system employing the SP demapper. The BER curve dips below 10^{-5} using a single iteration at E_b/N_0 =5.4dB. Upon employing I=4 iterations, the additional iteration-induced coding gain of the STBC-SP-MLC scheme becomes about 3.5dB at BER=10^{-5}.

Observe in Figure 7 that a single-class 1/2-rate STBC-SP-LDPC scheme having an effective throughput of 1 bit/channel use was also used for comparison with our MLC structure, where the MLC codes of Table 2 were replaced by the single-class LDPC(2560, 1280) scheme having a coding rate of 1/2. All LDPC component codes employed in our simulations used a total of five iterations for generating sufficiently reliable $extrinsic$ LLRs. The complexity of a single 2560-coded-bit LDPC code and that of the four 640-coded-bit MLC-LDPC component codes of Table 2 was deemed similar in these systems. More explicitely, the LDPC decoding complexity of each iteration associated with a parity check matrix having a column weight of j and row weight of k may be approximated in terms of the number of additions and subtractions in the logarithmic domain [16]. The corresponding BER results are shown in Figure 7.

Sphere packing modulation	Largest Min. Euclidean
Conventional modulation	16QAM, Ungerböck P.
MLC component output block length	640 bits
STBC-SP-LDPC output block length	2560 bits
No. of LDPC iterations	5
LDPC column weight	3
Total number of frame	5000
Overall system throughput	1 bit/channel use
Doppler frequency	0.1

Table 3: System parameters.

Our proposed STBC-SP-MLC system exhibits a similar BER performance to that of the single-class STBC-SP-LDPC structure characterized in Figure 7, although the proposed scheme has a slightly better performance at a low number of iterations. By contrast, the single-class scheme of Figure 7 performs approximately 0.45 dB better at a higher number of iterations at BER 10^{-5}. This is a consequence of the fact that each MLC component code has a four times lower codeword length compared to the single-class LDPC(2560, 1280) code. However, the advantage of using MLC is the employment of shorter individual LDPC component codes, hence potentially requiring a lower memory and having the flexibility of freely adjusting the coding rates compared to other coded modulation schemes, which is beneficial for example according to the typical requirements of high-quality, error-resiliant audio or video transmissions. Figure 8 shows the individual BER performance curves of the proposed STBC-SP-MLC scheme in comparison to the single-class STBC-SP-LDPC scheme. At I=2 iteration, all the bits in the single-class STBC-SP-LDPC scheme shows a similar BER performance. By contrast, the BER performance associated with each protection level of the proposed STBC-SP-MLC scheme becomes different.

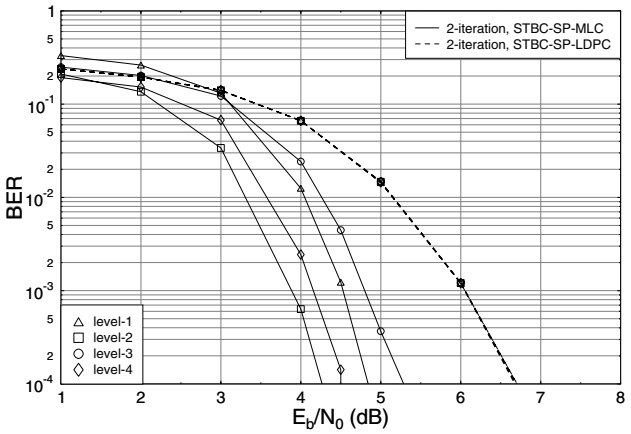

Figure 8: BER versus E_b/N_o performance of the STBC-SP-LDPC scheme using a single 1/2-rate component code LDPC(2560,1280) and having an effective throughput of 1 bit/channel use in comparison to the proposed STBC-SP-MLC scheme, when communicating over a correlated Rayleigh fading channel. Each bit protection level is shown as an individual BER curve.

5. CONCLUSIONS

In conclusion, a novel STBC-SP-MLC scheme was proposed. The scheme invokes a serially concatenated LDPC-based MLC arrangement combined with STBC using SP modulation. The MLC scheme was decoded in a multistage manner [1]. A useful equivalent capacity based design was proposed for determining the coding rates of each of the component codes in this scheme. This proves to be crucial for the sake of achieving the best attainable BER performance in conjunction with different SP mapping schemes designed for the 4D constellation space. Our simulation results outlined in Figures 5-8 characterize the achievable performance. We can observe from Figure 6 that at an effective throughput of 1 bit/channel use, the proposed STBC-SP-MLC scheme is capable of achieving an E_b/N_0 gain of about 3.5dB compared to the STBC-MLC benchmarker invoking classic 16QAM. Even though the proposed MLC-aided and the single-class STBC-SP-LDPC exhibit a similar performance, the multiclass scheme exhibits a higher flexibility and has the ability of providing an unequal error protection capability. Our future research will consider the design of different bit-to-SP-symbol mapping schemes for achieving unequal error protection with the aid the proposed equivalent capacity based design for determining individual component rates.

6. REFERENCES

[1] H. Imai and S. Hirawaki, "A New Multilevel Coding Method Using Error Correcting Codes," *IEEE Transactions on Information Theory*, pp. 371–377, May 1977.

[2] W. Su, Z. Safar, and K. J. R. Liu, "Space-Time Signal Design for Time-correlated Rayleigh Fading Channels," in *IEEE International Conference on Communications*, (Anchorage, Alaska), pp. 3175–3179, May 2003.

[3] M. Isaka, R. H. M-Zaragoza, M. P. C. Fossorier, S. Lin and H. Imai, "Multilevel Coded 16-QAM Modulation with Multistage Decoding and Unequal Error Protection," in *Global Communication Conference*, vol. 6, (Sydney, Austrialia), pp. 3548–3553, November 1998.

[4] L. H-J. Lampe, R. Schober and R. F. H. Fischer, "Multilevel Coding for Multiple-Antenna Transmission," *IEEE Transactions on Wireless Communications*, vol. 3, pp. 203–208, January 2004.

[5] D-F. Yuan, F. Zhang, A-F. So, Z-W. Li, "Concatenation of Space-Time Block Codes and Multilevel Coding over Rayleigh Fading Channels," in *IEEE Vehicular Technology Conference*, (Atlantic City, USA), pp. 192–196, October Fall 2001.

[6] S. M. Alamouti, "A Simple Transmitter Diversity Scheme for Wireless Communications," *IEEE Journal on Selected Areas in Communications*, vol. 16, pp. 1451–1458, October 1998.

[7] V. Tarokh, H. Jafarkhani and A.R. Calderbank, "Space-Time Block Codes from Orthogonal Designs," *IEEE Transactions on Information Theory*, vol. 45, pp. 1456–1467, July 1999.

[8] W. Su, Z. Safar, and K. J. R. Liu, "Space-Time Signal Design for Time-correlated Rayleigh Fading Channels," *IEEE International Conference on Communications*, pp. 3175–3179, May 2003.

[9] O. Alamri, B. L. Yeap, L. Hanzo, "Turbo Detection of Channel-Coded Space-Time Signals Using Sphere Packing Modulation," in *IEEE Vehicular Technology Conference*, (Los Angeles, USA), pp. 2498–2502, September Fall 2004.

[10] L. Hanzo, T. H. Liew and B. L. Yeap, *Turbo Coding, Turbo Equalisation and Space Time Coding for Transmission over Wireless channels*. New York, USA: John Wiley IEEE Press, 2002.

[11] U. Wachsmann, R. F. H. Fischer and J. B. Huber, "Multilevel Codes: Theoretical Concepts and Practical Design Rules," *IEEE Transaction on Information Theory*, vol. 45, pp. 1361–1391, July 1999.

[12] R. Gallager, *Information Theory and Reliable Communication*. New York: Willey, 1968.

[13] R. Gallager, *Low Density Parity Check Codes*. USA: MIT Press, 1963.

[14] J. H. Conway and N. J. Sloane, "Sphere Packings, Lattices and Groups," *Spinger-Verlag*, 1999.

[15] S. X. Ng and L. Hanzo, "On the MIMO Channel Capacity of Multi-Dimensional Signal Sets," *IEEE Transactions on Vehicular Technology*, vol. 55, pp. 528–536, March 2006.

[16] F. Guo, S. X. Ng and L. Hanzo, "LDPC assisted Block Coded Modulation for Transmission over Rayleigh Fading Channels," in *IEEE Vehicular Technology Conference*, vol. 3, (Florida, USA), pp. 1867–1871, April Spring 2003.